

Manuscript version: Author's Accepted Manuscript

The version presented in WRAP is the author's accepted manuscript and may differ from the published version or Version of Record.

Persistent WRAP URL:

<http://wrap.warwick.ac.uk/168862>

How to cite:

Please refer to published version for the most recent bibliographic citation information. If a published version is known of, the repository item page linked to above, will contain details on accessing it.

Copyright and reuse:

The Warwick Research Archive Portal (WRAP) makes this work by researchers of the University of Warwick available open access under the following conditions.

Copyright © and all moral rights to the version of the paper presented here belong to the individual author(s) and/or other copyright owners. To the extent reasonable and practicable the material made available in WRAP has been checked for eligibility before being made available.

Copies of full items can be used for personal research or study, educational, or not-for-profit purposes without prior permission or charge. Provided that the authors, title and full bibliographic details are credited, a hyperlink and/or URL is given for the original metadata page and the content is not changed in any way.

Publisher's statement:

Please refer to the repository item page, publisher's statement section, for further information.

For more information, please contact the WRAP Team at: wrap@warwick.ac.uk.

Optimizing RH refining process to maximize cleanliness of low-carbon low-silicon Al killed steel

Shuo ZHAO ^{1*}, Bing-shan WANG ¹, Shi-bin Zhu ¹, Gao-yang Song ¹, Shuai WANG ¹, Zu-shu Li ²

(1. Hebei High Quality Cold Heading Steel Innovation Technology Center, School of Materials and Science Engineering, Hebei University of Engineering, Handan 056000, Hebei, China;

2. WMG, University of Warwick, Coventry CV4 7AL, UK)

Abstract : In the LD (Linz Donawitz converter) – RH (Ruhrstahl Heraeus process) – CC (Continuous Casting) process for producing low-carbon low-silicon steel, the cleanliness level of slab was studied by optimizing the compositions of the refining slag and oxygen blowing flow in trial heats through judicious control. In order to realize RH without oxygen blowing, the oxygen content of molten steel should reach 475 – 525 ppm before RH degassing to guarantee that, the free oxygen is in the range of 100 - 150 ppm after the carbon-oxygen reaction. When the slag compositions was controlled to CaO = 41 – 50 wt.-%, Al₂O₃ = 29 – 36 wt.-%, SiO₂ = 5 – 11 wt.-% and MgO = 6 – 10 wt.-% in the RH treatment without feeding calcium, the total oxygen content in the plate was 18 ppm, and the nitrogen content decreased to 17 ppm in the improved process. The micro-inclusions in the slab mainly consisted of MgO-Al₂O₃-(MnS) and Al₂O₃-(MnS), and the particles size was mainly concentrated below 3 μm. The average total amount of large electrolytic inclusions in slab was 1.384 mg/ kg steel. The large inclusions were mainly SiO₂, Al₂O₃, SiO₂-Al₂O₃-(K₂O), and MgO-Al₂O₃.

Keywords: Castability; RH refining slag; Oxygen blowing; Inclusions; Low carbon low silicon steel

With the progress of science and technology and economic development, the requirements for steel quality have become more demanding. In the metallurgical industry, there has been an upsurge in research on steel quality control centered on reducing harmful impurities in steel and improving the cleanliness of steel [1-5]. At the same time, in order to improve the economic benefits, iron and steel enterprises strive to develop high- cleanliness and high- value- added products, such as automobile sheets, rare earth steel, pipeline steel, bearing steel, and other Al killed steel. These steels have strict requirements for [P], [S], T[O] (total oxygen content) and inclusions (including the size, morphology, distribution, etc.) [6-11].

In order to minimize the inclusions and sulfur content in clean steel, the basic metallurgical requirement is that the molten steel should be adequately reduced, that is, low oxygen activity in steel is beneficial to desulfurization. Therefore, in the traditional steelmaking process, the molten steel is deeply deoxidized during converter tapping. When the oxygen content becomes very low, desulfurization is completed by the slag-steel reaction. Although this process can afford molten steel with a very low [S] content, deoxidized products such as SiO₂ and Al₂O₃ generated by deep deoxidation remain in the molten steel, which often become inclusions in billets and products, making it difficult to obtain high-cleanliness billets [12-18]. In order to overcome the above

disadvantages of the traditional steelmaking process, in the enterprises with RH equipment, the molten steel is not deoxidized or is weakly deoxidized during the tapping process in the converter, and enters the RH vacuum degassing unit after heating [19]. The [C] – [O] reaction is used to deoxidize steel, where the molten steel is deoxidized without or with little Al in the treatment process. The amount of deoxidized alloy is reduced, and the oxide inclusions are reduced, which is beneficial for improving the cleanliness of molten steel, simplifying the production process, and reducing the cost.

In a reconstructed city steel plant, low- carbon or ultra- low- carbon and, low- silicon steel are produced by the new process of weak deoxidization during converter tapping → argon blowing → carbon-oxygen reaction in RH → continuous casting. Despite explorations and improvements for actual production, the cleanliness index of molten steel is still poor, and the T[O] content and large inclusions in steel remain high, which does not meet the cleanliness requirements for high- quality cold- rolled sheets. It is necessary to further stabilize the refining process, improve the cleanliness of molten steel, and evaluate the cleanliness level of rolled steel. The process developed herein has positive significance for reducing the amount of deoxidized alloys in molten steel, reducing the residual oxide inclusions in molten steel, simplifying the refining operation and reducing the production cost.

1 Basic conditions for controlling steel grade

1.1 Chemical compositions

The chemical composition ranges based on the steel grade are shown in Table 1. In actual production, when [C] is controlled within the range of 0.02 – 0.04 wt.-%, the sensitivity of longitudinal cracks on the slab surface is only inferior to that of peritectic steel, Thus, in order to reduce the longitudinal crack ratios of the slab surface, [S] and [P] are usually controlled to below 0.015 wt.-% and 0.020 wt.-%, respectively.

Table 1 Chemical composition of low carbon low silicon steel / wt-%

C	Si	Mn	Al _s	S	P	Ni	Cr
≤0.050	≤0.030	0.18~0.22	0.020~0.070	≤0.020	≤0.023	≤0.10	≤0.10

1.2 Use and delivery status of steel

The target steel is a high- quality carbon structural steel. It is a typical steel with low carbon, low silicon, and high acid- soluble aluminum content. Its yield strength is not less than 270 MPa. It exhibits good plasticity, toughness, deformability, and weldability. It is fabricated by using a hot- rolled coil or cold- rolled coil, and applied in the following fields: ① automobile industry, the main uses include: automobile chassis system, wheel, cab interior panel, carriage plate, other stamping parts: bumpers, brake pads and other small parts inside the car; ② mechanical industry; ③ light industrial appliances.

2 Production process and existing problems

When the amount of slag present during converter tapping is large, the reaction of steel-slag is sufficient, and the steel-slag in the ladle furnace (LF) is fully stirred and contacted, which will lead to the reduction of SiO_2 in slag by $[\text{Al}]$ in steel, resulting in an increase in the amount of silicon in the molten steel, which may even surpass the composition range. Therefore, in producing the target steel, the amount of converter slag should be reduced as much as possible, and LF treatment should be avoided as much as possible. The scheme for the production process in a certain plant is as follows: Blast furnace \rightarrow Kambara reactor desulfurization \rightarrow Converter smelting \rightarrow Tapping and alloying \rightarrow RH refining \rightarrow Continuous casting \rightarrow Slab rolling. The required $[\text{C}]$ content in molten steel is less than 0.04 wt.-%. In order to prevent serious peroxidation of molten steel and shortening of the lining life caused by low-carbon tapping in the converter, the deoxidation degree should be as low as possible during tapping, while the deoxidation should be carried out at the same time as RH decarbonization.

In this process, the excess oxygen can be largely removed during the $[\text{C}] - [\text{O}]$ reaction in the RH, and the endpoint $[\text{C}]$ in the converter is allowed to be high to reduce excess oxygen and improve the lining life. In addition, the reactivity between ladle slag and molten steel during RH treatment is weak, and the excessive $[\text{Si}]$ content can be avoided. Therefore, this process is also chosen as the main refining mode in production. The key is that after RH primary deoxidation, when Al is added for final deoxidation and alloying, the main deoxidation product is Al_2O_3 . If the deoxidation products are not fully removed or modified, aggregation of the inclusions in molten steel occurs readily, which blocks the nozzle. In the casting process, a protective casting is strictly required. Therefore, the following problems often exist in production:

(1) In the original process, the intensity of argon stirring at the ladle bottom is not sufficient during converter tapping, and the melting capacity of the composite slag is poor, resulting in a weak reduction effect when the reducing agent is added; thus, the oxidation of top slag after RH treatment remains high. The refining slag before RH treatment has a high melting point of $1600\text{ }^\circ\text{C}$, in the region between that of $2\text{CaO}\cdot\text{SiO}_2$ and $3\text{CaO}\cdot\text{SiO}_2$. According to the literature^[20], the high melting point of refining slag leads to slow melting of the slagging agent during tapping, which is not conducive to the absorption of inclusions. In addition, slag washing is inefficient due to the short tapping time. In this way, it is easy to block the submerged nozzle or long shroud at the end of the ladle casting. Thus, the casting of molten steel often becomes difficult when the residual steel in the ladle is about 30 ton.

(2) In the early stage of production, due to the instability of the ironmaking production rhythm and liquid iron input in the converter, the RH temperature fluctuates greatly at the beginning, which makes it necessary to increase the temperature by adding Al. At the end of oxygen blowing and carbon reduction, the excess oxygen and final slag oxidation in the steel are higher, and more Al_2O_3 inclusions are formed in the Al final deoxidation process. Moreover, because the heating time is extended, the RH vacuum time after the final deoxidation with added Al is not sufficient based on the required rhythm, and the removal of Al_2O_3 is not sufficient; thus, poor pourability easily results.

In summary, due to the large number of inclusions in steel and the unstable castability of molten steel, nozzle clogging and excessive argon blowing often occur in the original process, resulting in defects on the slab surface. As a result, the slab must be subjected to offline inspection and cleaning, and cannot meet the requirements for casting- rolling compact layout and hot delivery- hot charging.

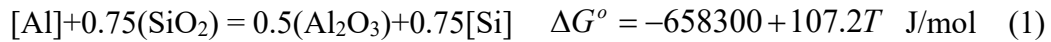
3 Optimization of refining process

3.1 Improvement of refining slag

In order to ensure the free oxygen activity required for RH decarburization during actual production, for low- carbon low- silicon steel, the weak deoxidation process is mainly adopted during tapping, and the $[Al_3]$ content in the molten steel is relatively low. The steel can be deoxidized by $MnFe + AlFe$ or $AlMnFe$, where the deoxidation products are Al_2O_3 and a small amount of MnO . In the design of refining slag, the melting capacity should be considered first, after which the ability to assimilate and absorb of Al_2O_3 and spinel should be considered in order to improve the efficiency of inclusion removal. Finally, the sulfur capacity should be set to a higher level. In the RH refining process, a strong argon blowing rate and sufficient vacuum treatment time are required to ensure efficient floating removal of low melting point inclusions.

At the end of the decarburization reaction, the Al added in the final deoxidation and alloying, process easily reacts with the molten steel components or oxidizing substances (FeO , MnO and SiO_2) in the slag to form Al_2O_3 inclusions with high melting points. The reduction and desulfurization reactions between steel and slag in the refining process are described as follows^[21]:

① Steel- slag reduction reaction:



② Desulfurization reaction :



The Gibbs free energy isothermal equation is as follows: $\Delta G = \Delta G^\circ + RT \ln J$, where. ΔG° is the Gibbs free energy of the system in the standard state, and J is the activity ratio of the substances in the actual state. When $\Delta G = 0$, the reaction is in the equilibrium state. The positive and negative values of ΔG represent the reaction direction. Therefore, in order to inhibit the steel- slag reaction to form high- melting-point inclusions, the necessary condition is $\Delta G > 0$; to improve the slag desulfurization capacity, the necessary condition is $\Delta G < 0$.

Similarly, the composition of the refining slag should be tailored to the actual situation for producing low- carbon low- silicon steel by considering the following principles ^[22,23]:

① Accord to thermodynamic calculation results, in order to inhibit the reaction between $[Al]$ and top slag after tapping, it is necessary to satisfy $a_{(Al_2O_3)}^{0.5} / a_{(SiO_2)}^{0.75} > 105.7$, that is, to increase Al_2O_3 in refining slag by more than 28 wt.-% and to control SiO_2 below

12 wt.-%. In addition, converter slag and auxiliary materials will bring in not less than 5 wt.-% SiO₂ into the slag, a certain amount of SiO₂ is conducive to reducing the melting point of converter slag.

②When CaO/Al₂O₃ ratio of refining slag is 1.4 - 1.7, it has good deoxidation and desulfurization ability, and the average sulfur distribution ratio can reach more than 100. When the ratio of CaO/Al₂O₃ content is too large, the melting temperature of refining slag will continue to increase, affecting the slag formation rate. If the ratio of CaO/Al₂O₃ is too low, the ability of refining slag to absorb Al₂O₃ will be weakened.

③Adding 6 wt.-% MgO in slag can protect lining and reduce erosion. MgO in the slag should not be too high, generally 6 wt.-% to 10 wt.-%, otherwise the alkalinity is too high, the formation of high melting point periclase in the slag is difficult to melt.

④CaF₂ in slag is not more than 5 wt.-% due to a small amount of fluorite in the auxiliary material.

The target composition of refining slag is shown in Table 2.

Table 2 Target range of refining slag, wt.-%

CaO	Al ₂ O ₃	SiO ₂	MgO	CaF ₂	Melting point range	Viscosity,1500°C
41 - 50	29 - 36	5 - 11	6 - 10	<5	<1500°C	0.35 - 0.46Pa·s

3.2 Suitable oxygen blowing flow for RH decarburization

In order to ensure smooth RH decarburization during steel production, after reducing the oxidizability of the top slag, it is still necessary to supply external oxygen for decarburization. If the oxygen blowing volume is too large, the oxygen content in steel will be too high after decarburization. Thus, more Al will be required for deoxidization, and the amount of inclusions in the steel will increase. At the same time, Al₂O₃ inclusions floating into RH refining slag will make inclusion removal difficult.

Table 3 Oxygen content and consumption at each process step

No.	Liquid steel weight/t	$a_{[O]}$ before RH/ppm	$a_{[O]}$ after adding C/ppm	Oxygen blowing volume/m ³	Adding Al weight/kg	[C] before RH/%	[C] after RH/%	Oxygen consumed by C /ppm	Oxygen consumed by Al /ppm	Oxygen from slag/ppm
1#	218.9	287	109	120	248	0.04	0.02	266.67	1007.06	312.59
2#	230.9	281	66	100	200	0.05	0.01	533.33	769.93	469.57
3#	215	433	82	100	214	0.07	0.02	666.67	884.75	535.97
4#	224	450	257	80	168	0.03	0.01	266.67	666.67	230.13
5#	226.6	372	56	60	120	0.04	0.02	266.67	470.73	43.13
6#	226.2	455	227	60	120	0.03	0.01	266.67	471.56	131.29
7#	215.5	316	70	60	116	0.04	0.01	400.00	478.47	234.73
8#	221.3	422	275	50	100	0.03	0.01	266.67	401.67	198.57
9#	225	453	238	50	100	0.05	0.01	533.33	395.06	395.93

The oxygen content at each process step is shown in Table 3. From the experimental data, when the oxygen blowing volume is 60m³, the content of Σ (FeO) in the initial slag is low; thus, the oxygen supply from the slag to molten steel is low, at only 43.13 ppm. According to the calculated data summarized in Table 3, the average weight of liquid steel is 222.6 t, the weight of added Al is 70 kg, the average [C] at the

beginning and at the ending is 0.042 and 0.013 %, respectively, and the average oxygen supply from slag is 283.5 ppm. In order to ensure that the free oxygen activity of molten steel after adding C is within the range of 100 – 150 ppm, the appropriate oxygen blowing volume can be calculated as shown in Figure 1. To achieve no oxygen blowing during RH production, when the free oxygen activity is controlled to 100 ppm, the oxygen activity of molten steel before RH treatment should be greater than 475 ppm, and when the free oxygen activity is controlled to 150 ppm, the oxygen activity before RH treatment should be greater than 525 ppm.

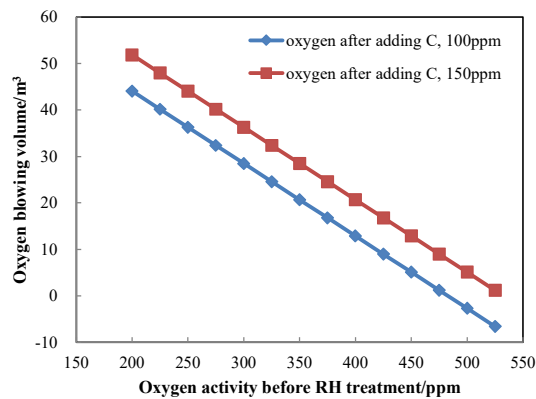


Fig. 1 Relation of the oxygen blowing volume and the oxygen activity before RH treatment

4 Application

4.1 Cleanliness level of molten steel under original RH process

4.1.1 Castability and clogging analysis of molten steel

(1) Castability of molten steel

The original process is RH vacuum treatment with blowing oxygen. The castability of molten steel can be judged based on the production records for a continuous casting machine tracked on site, combined with the change in the degree of stopper opening in Fig. 2. The degree of stopper opening increased as the casting time became longer. From the starting of a new casting ladle to the normal casting break, nozzle clogging continuously increased, and the stopper position increased by about 15 – 20 mm.

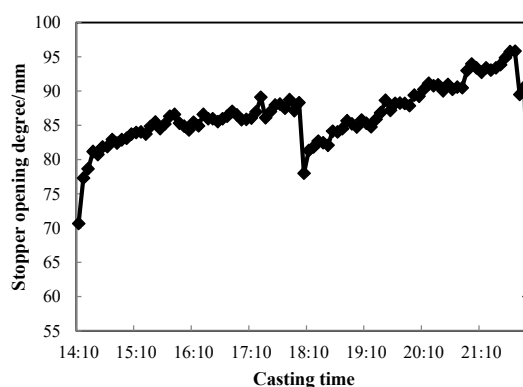


Fig. 2 Change curve of stopper opening degree during casting process

(2) Components contributing to nozzle clogging

The cloggings in the submerged nozzles (heat No. 21B218 and 23C796) were stripped and pulverized into powders. The powder compositions determined by X-ray diffraction (XRD) analysis are shown in Fig. 3. The main chemical component of the clogging in the submerged nozzle was Al_2O_3 , along with a small amount of $\text{CaO}\cdot 6\text{Al}_2\text{O}_3$, Fe_3O_4 , and $\text{MgO}\cdot\text{Fe}_2\text{O}_3$.

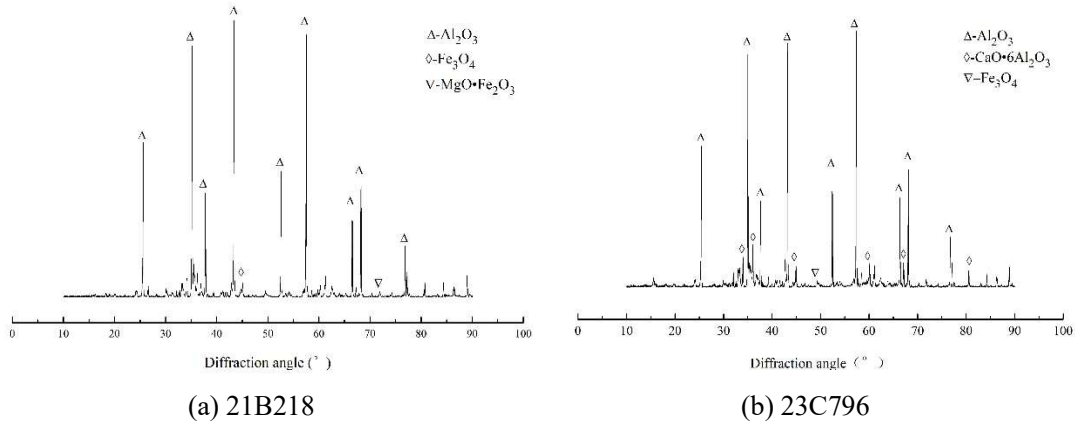


Fig. 3 XRD analysis of cloggings

4.1.2 Number, morphology, and composition of micro-inclusions in liquid steel

In order to investigate the morphology of the inclusions in molten steel in the original process, five heat samples were taken from the start of RH, end of the RH, and tundish in normal casting production. The type and size distribution of the micro-inclusions in steel manufactured by the original LD - RH - CC process were analyzed:

(1) The number of inclusions before RH treatment was 37.1 mm^{-2} , indicating that most of the oxygen in steel was in the form of inclusions 3 min after entering the RH station, and the free oxygen content was low. At the end of vacuum treatment, most of the Al_2O_3 generated during the Al final deoxidation had not been removed, and the number of inclusions increased to 51.6 mm^{-2} when leaving the station. Because the flow of molten steel was controlled properly in the tundish, the number of inclusions was significantly reduced to 19.17 mm^{-2} . The metallographic analysis showed that there was no obvious change in the size of inclusions in each process. The increase in the number of 2.5 - 5 μm inclusions after RH treatment was consistent with the number density. Because the inclusions in molten steel float easily as the size increases, the size distribution of the inclusions in the tundish was generally $< 5 \mu\text{m}$, accounting for about 77%. Inclusions with sizes of 5 - 10, 10 - 30, and $> 30 \mu\text{m}$ accounted for 20, 2, and 1% of the total inclusions, respectively.

(2) The inclusions before RH treatment were mainly primary deoxidation products of Si and Al, such as Al_2O_3 , SiO_2 , and a small amount of MgO. The Al_2O_3 inclusions generally had an irregular shape, with size of $\leq 15 \mu\text{m}$. In addition to Al_2O_3 , SiO_2 and $\text{MgO}\cdot\text{Al}_2\text{O}_3$, $\text{Al}_2\text{O}_3\text{-FeS}$ composite inclusions were found after RH treatment. The Al_2O_3 inclusions were globular, with sizes of $\leq 5 \mu\text{m}$. The SiO_2 inclusions had sizes of $\leq 40 \mu\text{m}$, with spherical, blocky, rod-like and other shapes. The types of micro-inclusions in the tundish were basically the same as those after RH treatment, but the

number of final Al_2O_3 deoxidation products increased significantly. The $\text{MgO-Al}_2\text{O}_3$ inclusions had sizes of $\sim 20 \mu\text{m}$, and the size of the SiO_2 and Al_2O_3 inclusions was generally within $10 \mu\text{m}$. The results indicate that the RH slag or tundish covering agent had weak ability to adsorb smaller SiO_2 and Al_2O_3 particles, and the steel also contained fine Al_2O_3 -sulfide composite inclusions after RH treatment. Thus, the desulfurization capacity of the refining slag should be strengthened, the RH oxygen blowing volume should be reduced, and the pretreatment conditions should be improved.

4.2 Experimental results for optimizing RH refining process

4.2.1 Castability control of molten steel

The refining process for RH without oxygen blowing was optimized through continuous experiments, the refining process optimization experiments were carried out continuously, and the casting process was tracked from the first heat in the new casting sequence. The 13 heat casting curves for molten steel are shown in Fig. 4.

The tundish nozzle was changed once in the 7th heat, the inside of the nozzle was relatively smooth (Fig. 5), no large clogging could be found, the casting situation was ideal, the stopper remained stable, there was only a slight rise of the stopper at the casting end, indicating that the Al_2O_3 absorption capacity of the refining slag was enhanced, the inclusions decreased significantly, and clogging slowly accumulated in a small part as the casting time was extended; finally, a slight rise in the stopper position was observed. The comprehensive change in the stopper and casting speed reflects improved castability of the molten steel refined by RH, where no nozzle change is required for at least 7 heats.

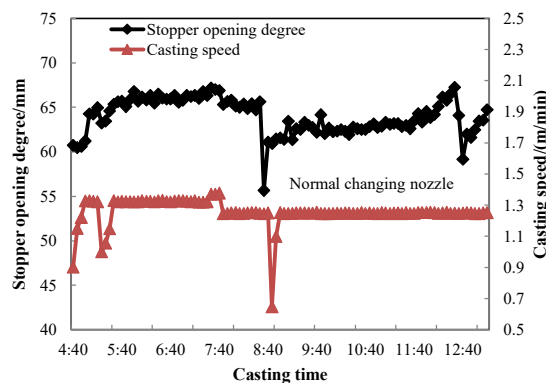


Fig. 4 Stopper curve during continuous casting



Fig.5 Replaced nozzle in tundish

4.2.2 Analysis of composition of molten steel and refining slag

(1) Composition control of molten steel and refining slag

The change in the $[\text{Al}]$ content of the steel in moving from the Ar blowing station to the tundish is shown in Fig. 6. The composition of molten steel after tapping was analyzed, indicating that the $[\text{Al}_s]$ in molten steel in the Ar blowing station was 0.004 – 0.014 wt.-%, the $[\text{Al}_s]$ in the molten steel after RH treatment was 0.032 – 0.038 wt.-%, the $[\text{Al}_s]$ in the molten steel in the tundish was 0.019 – 0.030 wt.-%, where $[\text{S}] = 0.007$ – 0.013 wt.-%. The $[\text{Al}_s]$ in molten steel first increased and then decreased. After the RH cycle for 3 min, the $[\text{Al}_s]$ content reached the lowest value. After Al deoxidation and alloying, the $[\text{Al}_s]$ content increased rapidly in the middle and ending of the RH.

Thereafter, the aluminum loss in the process from the RH to tundish was quite serious, reaching 0.011 wt.-%. Therefore, in order to control the casting heats of molten steel, it was necessary to reduce the generation of Al_2O_3 at the ending of RH. Thus, strict protective measures such as “sealing ring + Ar blowing” were implemented for long nozzle during ladle casting.

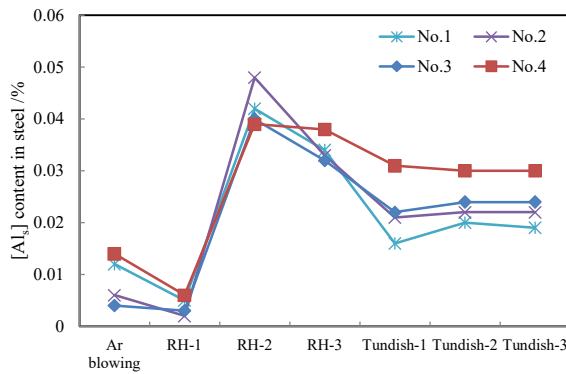


Fig 6 Control of $[\text{Al}_s]$ in steel

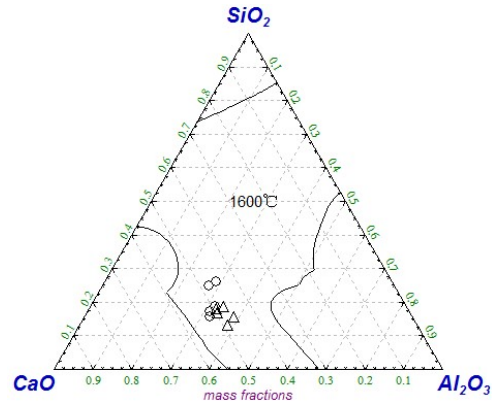


Fig. 7 Composition control of refining slag (○before RH, △after RH)

Figure 7 shows that the composition change of refining slag at the starting and ending of the RH furnace. After RH vacuum treatment, the SiO_2 content in the slag decreased, the CaO content basically remained unchanged, and the Al_2O_3 content increased significantly. On one hand, these changes indicate that the slag had strong adsorption capacity for Al_2O_3 ; on the other hand, in order to reduce the reaction between $[\text{Al}]$ and top slag under vacuum conditions, it was necessary to strictly control the amount of slag from the converter and the SiO_2 introduced by the raw material.

(2) T[O] and [N] content in steel

The change in the oxygen and nitrogen content in each process is shown in Figs.8 - 9. The average T[O] content after RH treatment was 37 ppm; T[O] content in the slab and plate was 22 ppm and 18 ppm, respectively. The average [N] content after RH treatment was 18 ppm; the [N] content in the slab and plate was 19 ppm and 17 ppm, respectively.

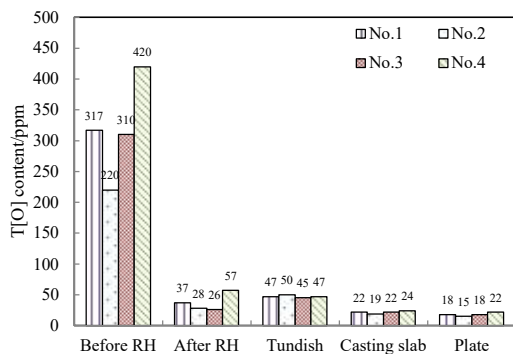


Fig 8 Change of T [O] content in steel

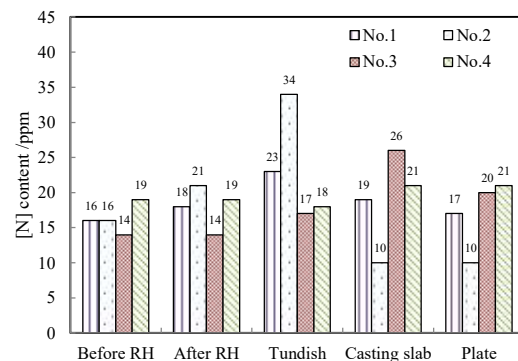


Fig. 9 Change of [N] content in steel

As shown in Figs. 8 and 9, after optimizing the refining slag system, the T[O] before RH treatment was reduced by 11.5 % compared with that before optimization. Most of the inclusions floated to the top slag after vacuum circulation of the molten

steel. Upon completion of the RH treatment, the T[O] in the molten steel was greatly reduced (by 86.4 %), and the vacuum degassing effect was obvious. The [N] removal rate in molten steel was 34 % at the start of the RH furnace (3 min before vacuum circulation), but there was not obvious change in the [N] content of molten steel during RH treatment; the T[O] and [N] in molten steel increased to 4 ppm and 5 ppm, respectively, after RH treatment. The T[O] content in molten steel after refining was related to the T[O] content before RH treatment, oxidation of the top slag, and the components of the tundish covering agent. The Ar sealing effect of the long nozzle will also directly determine if the nitrogen increase is significant or not.

4.2.3 Quantitative evaluation of inclusions in each process

One-hundred-and-fifty fields of view were observed continuously under $500\times$ magnification by using a metallographic microscope. Image-Pro Plus was used to determine the number density, area, and size distribution of the inclusions in each field of view. The metallographic statistical results are shown in Figs. 10 and 11.

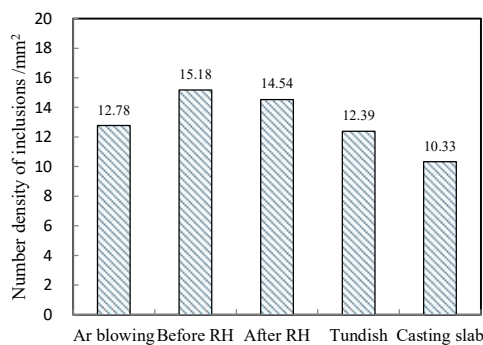


Fig 10 Number density of inclusions in steel of each process

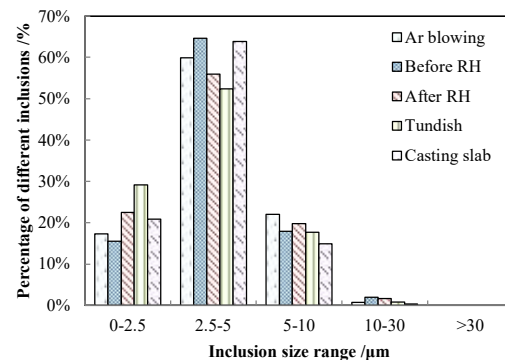


Fig. 11 Size distribution of inclusions in steel in each process

After RH oxygen blowing and optimization of the refining slag, the number density of inclusions in the Ar blowing station was relatively low, only 12.78 mm^{-2} . In order to reduce the oxidation of top slag, Al powders were sprayed on the slag surface for deoxidization, and some Al_2O_3 entered the molten steel through interface diffusion. Therefore, the number density of inclusions was 15.18 mm^{-2} when entering the RH station, which is a slight increase. During the subsequent process, the number of inclusions decreased, and the number density of inclusions in the slab decreased to 10.33 mm^{-2} . Due to diffusion deoxidization and carbon deoxidization under vacuum conditions, the number of large inclusions was greatly reduced. No inclusion larger than $30\text{ }\mu\text{m}$ was found during the entire production process, and the inclusion number density was controlled at a low level. The inclusions with sizes of $5 - 10\text{ }\mu\text{m}$ and $10 - 30\text{ }\mu\text{m}$ decreased gradually, accounting for 14.9 % and 0.4 %, respectively, whereas the inclusions with sizes $\leq 5\text{ }\mu\text{m}$ increased gradually, accounting for 84.7 %. The main reason is that some of the Al particles were incorporated into the molten steel by deoxidation and alloying before leaving the station. Due to the relatively smaller particles, the deoxidation products did not comply with the Stokes theorem very well during floating; thus, they were retained in the molten steel. Therefore, many $\leq 5\text{ }\mu\text{m}$ inclusions remained in the slab.

4.2.4 Morphological and compositional changes of micro-inclusions in steel

(1) Inclusions in Ar blowing station

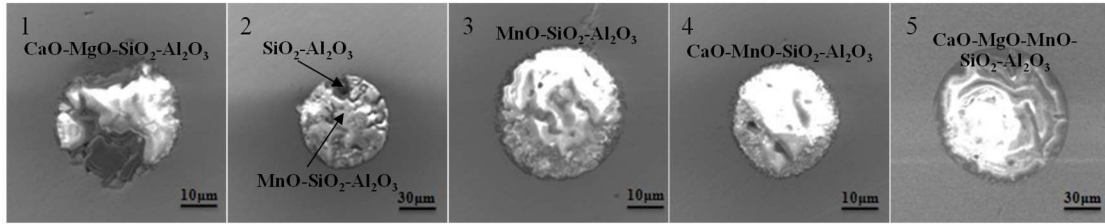


Fig 12 Morphology of typical inclusions in Ar blowing station

A weak deoxidation process was used during tapping. According to the composition in Fig. 12, it was determined that the inclusions were large spherical CaO-MgO-SiO₂-Al₂O₃ and MnO-SiO₂-Al₂O₃ systems with sizes of 20 - 50 µm, which are formed because the probability of collision between the deoxidation products and fine slag droplets increased by hundreds of times in the slag washing process. Most MnO-SiO₂-Al₂O₃ was formed as a composite deoxidation product and was adsorbed and aggregated by the slag to form larger inclusions. However, due to the short tapping time, the large inclusions could not all float into the slag layer, and some were retained in the molten steel.

(2) Inclusions before RH treatment

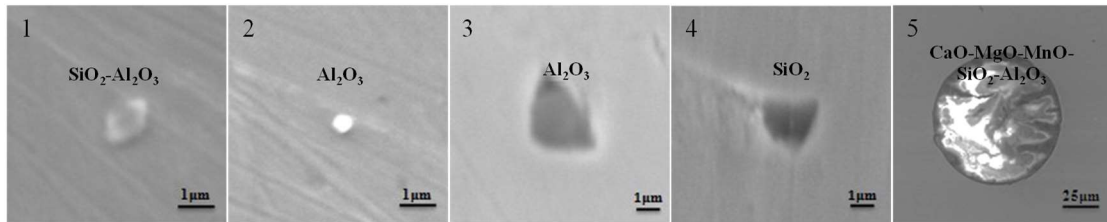


Fig.13 Morphology of typical inclusions before RH treatment

The inclusions in steel were mainly less than 3 µm SiO₂, Al₂O₃, and SiO₂-Al₂O₃ inclusions, according to the composition in Fig. 13, which were modified by adding Al powders to the top slag and stirring by argon blowing for 3 min when entering the RH station. Only a few large CaO-MgO-SiO₂-Al₂O₃ inclusions did not float. Although the free oxygen activity in the steel was still high, the number of large CaO-MgO-SiO₂-Al₂O₃ inclusions was significantly reduced.

(3) Inclusions after RH treatment

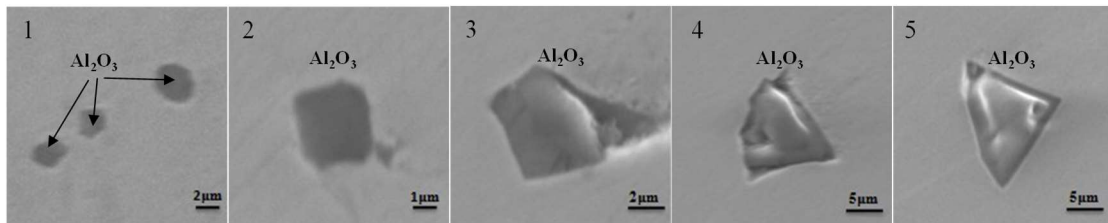
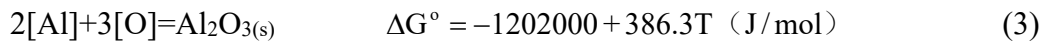


Fig. 14 Morphology of typical inclusions after RH treatment

Based on Fig. 14, the large inclusions essentially disappeared when the ladle left the RH station. The deoxidized products in steel were mainly ≤ 10 µm Al₂O₃ and SiO₂. The Al₂O₃ particles had round, square, and polygon shapes, and some of them existed as clusters. Due to the Al final deoxidation and alloying after vacuum treatment, fine Al₂O₃ inclusions were mostly formed at this step. If the soft blowing time was too

short or the caster production rhythm was tight, these inclusions could not be removed completely.



(4) Inclusions in tundish

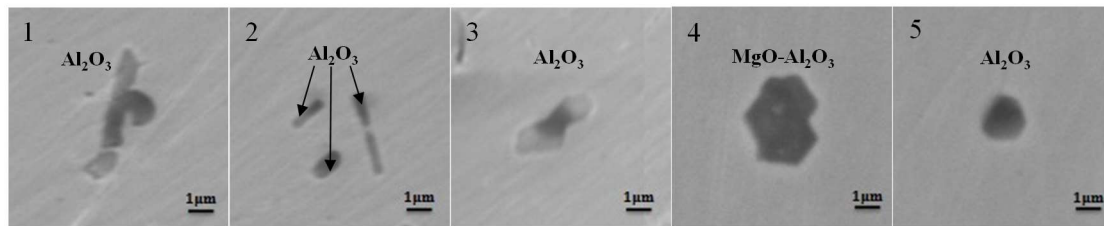


Fig.15 Morphology of typical inclusions in tundish

From Fig. 15, it is deduced that the main inclusions in the tundish were Al_2O_3 , which is basically the same as that in RH, and the inclusion size was further reduced to $\leq 5 \mu\text{m}$. Only a small amount of $\text{SiO}_2\text{-Al}_2\text{O}_3$, $\text{MgO-Al}_2\text{O}_3$, and $\text{MnO-Al}_2\text{O}_3$ inclusions was found, indicating that under the action of the turbulence inhibitor and retaining wall, the residence time of the molten steel in the tundish and the volume of the piston flow increased; the possibility of aggregation of the residual micro-inclusions also increased, and the large inclusion particles continued to float.

(5) Inclusions in slab

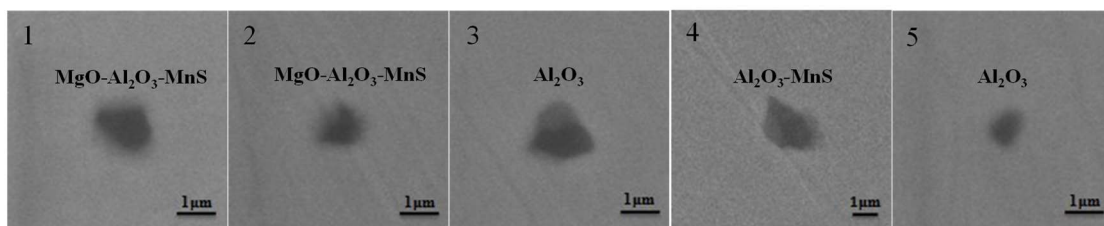


Fig.16 Morphology of typical inclusions in slab

The data in Fig. 16 show that all the inclusions in the slab were $\leq 3 \mu\text{m}$ $\text{Al}_2\text{O}_3\text{-(MnS)}$ and $\text{MgO-Al}_2\text{O}_3\text{-(MnS)}$, which had little effect on the slab quality. The small Al_2O_3 inclusions were not only derived from the deoxidation products generated during the refining process, but mainly from the secondary oxidation inclusions formed during the casting process. When molten steel flowed from the ladle nozzle to the mould, it was inevitable to inhale a part of the air, which would lead to the secondary oxidation of molten steel and precipitate more inclusions. Especially when the secondary oxidation of molten steel was serious, it might affect the castability of molten steel. According to the calculation results of inclusion precipitation during continuous casting, it can be found that Al_2O_3 was mainly precipitated during the cooling process of aluminum-containing steel. The estimated precipitation amount per kg of molten steel was shown in Table 4.

Table 4 Precipitation of Al_2O_3 at different temperatures and different oxygen contents

Oxygen inhalation volume	Nozzle temperature, 1550°C	Liquidus temperature, 1530°C
0 ppm	3.27 mg/kg steel	4.07 mg/kg steel
10 ppm	24.52 mg/kg steel	25.32 mg/kg steel
20 ppm	45.77 mg/kg steel	46.57 mg/kg steel

30 ppm

67.02 mg/kg steel

67.82 mg/kg steel

From the calculation results of Table 4, it can be seen that only Al_2O_3 precipitated during the cooling process of molten steel. In the absence of secondary oxidation, the amount of precipitation per kg of molten steel was very small, but in the presence of secondary oxidation, the amount of precipitation would be greatly increased, depending on the effect of protective casting on site. Therefore, in order to greatly reduce the number of small inclusions, it was not enough to optimize the deoxidization alloying system, argon blowing system, refining slag composition, etc., and it was necessary to strengthen the protective casting on site.

Sulfides were the main reaction products of the alloying elements and sulfur in steel. $\text{MgO-Al}_2\text{O}_3$ was related to the spalling and erosion of refractories. According to statistical analysis, the sources of the micro-inclusions were: deoxidized products or secondary oxidation products > sulfide > refractory corrosion products.

4.2.5 Morphology and composition of large inclusions in steel

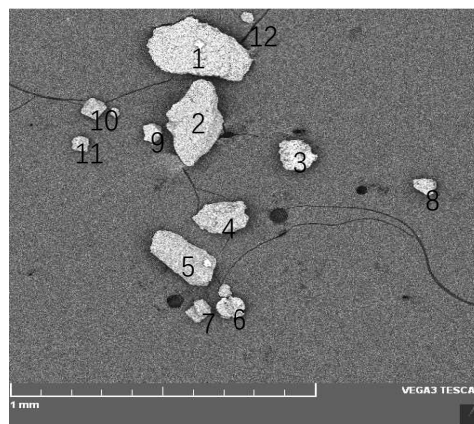


Fig.17 Morphology of large inclusions in slab

For RH without oxygen blowing, the total amount of electrolytic inclusions in the two slabs were 1.325 mg/kg steel and 1.442 mg/kg steel respectively, with an average of 1.384 mg/kg steel. Most of the large inclusions had a square morphology (Fig. 17). Combined with the data from the energy dispersive spectra of the inclusions (Table 5), the inclusions in steel were mainly SiO_2 , Al_2O_3 , $\text{SiO}_2\text{-Al}_2\text{O}_3\text{-(K}_2\text{O)}$, $\text{MgO-Al}_2\text{O}_3$. The SiO_2 , Al_2O_3 and $\text{SiO}_2\text{-Al}_2\text{O}_3$ inclusions were mainly deoxidation products or secondary oxidation products in molten steel, and magnesium aluminate was a combination of ladle slag or tundish coating materials (mainly composed of MgO) or alumina.

Table 5 Composition of inclusions in slab (wt.-%)

Inclusion	SiO_2	Al_2O_3	MgO	K_2O	Nb_2O_5	ZnCl_2	CaS
1	64.61	13.69		6.37	15.33		
2	100.00						
3		70.60				6.90	22.50
4-5	100.00						
6		68.11	31.89				
7		100.00					
8	82.22	17.78					
9	68.56	17.07		14.37			

10		100.00	
11	87.36		12.64
12		72.03	27.97

5 Conclusions

(1) When the free oxygen content in molten steel reached 475 – 525 ppm before RH treatment, it could be guaranteed to be 100 – 150 ppm after carbon deoxidation, which is beneficial for decreasing oxygen consumption and reducing the formation of inclusions. In order to ensure a stable level of liquid steel in the ladle during vacuum treatment, the oxygen blowing flow should be minimized. The suitable compositional range of refining slag should be controlled to: CaO = 41 – 50 wt.-%, Al₂O₃ = 29 – 36 wt.-%, SiO₂ = 5 – 11 wt.-%, MgO = 6 – 10 wt.-%.

(2) By optimizing the composition of the refining slag and RH oxygen blowing flow, the castability of low- carbon low- silicon steel could be improved. Under RH without oxygen blowing, molten steel could be cast continuously without nozzle clogging. The average T[O] content was 18 ppm in the plate, and the [N] content was 17 ppm. Metallographic analysis showed that the inclusion size was less than 30 μm. The < 5, 5 – 10, and 10 - 30 μm inclusions accounted for 84.7, 14.9, and 0.4 % of the total inclusions, respectively. The micro-inclusions in the slab were all ≤ 3 μm Al₂O₃-(MnS) and MgO-Al₂O₃-(MnS), which had little effect on the slab quality.

(3) The average total amount of electrolytic inclusions in the slab was 1.384 mg/kg steel. The large inclusions in steel were mainly SiO₂, Al₂O₃, SiO₂-Al₂O₃-(K₂O), and MgO-Al₂O₃, with square shapes. SiO₂, Al₂O₃, and aluminosilicate were mainly deoxidation products or secondary oxidation inclusions in molten steel, and spinel was a combination of ladle slag or tundish coating shedding products or alumina.

Acknowledge

Thanks for the support and assistance of the National Natural Science Foundation of China (51904086, 51904085), Returned Overseas Scholars Foundation of Hebei Province (C20200310), Talent Introduction Project of Hebei Province and Science and Technology Special Program of Handan City (19422111008-33).

Conflict of Interest

The authors declare that they have no known competing financial interests or personal relationships that could have appeared to influence the work reported in this paper.

References

- [1] N. Liu, G. Cheng, L. F. Zhang, W. Yang, Y. Ren, G.C. Wang. Composition evolution and deformation of different non-metallic inclusions in a bearing steel during hot rolling. *J. Iron Steel Res. Int.* 2022,29(4): 552-562.

- [2] S. Zhao, L. Ma, T. Yan, et al. Effect of different refining slag systems on cleanliness of molten steel for carbon structural steel. *J. S. AFR. I. Min. Metall.*, 2017, 117(4): 343-350.
- [3] Y. Wang, W.F. Li, W. Yang. Evolution of inclusions in a pipeline steel during continuous casting and hot rolling process. *J. Iron Steel Res. Int.* 2022,29(1): 175-185.
- [4] L. Cao, G.C. Wang, Y.Y. Xiao, R.G. Yang. Effect of Mg addition on TiN inclusions in GCr15 bearing steel. *J. Iron Steel Res. Int.* 2022,29(6): 925-938.
- [5] S. B. Venkata, R. P. Srinivasa and R. P. Govinda. Experimental investigation on influence of electrode vibrations on hardness and microstructure of 1018 mild steel weldments. *W. J. Eng.*, 2020,17(4): 509-517.
- [6] Y. Wang, C.R. Li, L.Z. Wang, X.Q. Xiong, L. Chen. Effect of yttrium treatment on alumina inclusions in high carbon steel. *J. Iron Steel Res. Int.* 2022,29(4): 655-664.
- [7] H. Matsuura, C. Wang, G. H. Wen and S.Sridhar. The transient stages of inclusions evolution during Al and/or Ti additions to molten iron. *ISIJ Int.* 2007, 47(9): 1265-1274.
- [8] G.X. Qiu, D.P. Zhan, L. Cao, H.S. Zhang. Effect of zirconium on inclusions and mechanical properties of China low activation martensitic steel. *J. Iron Steel Res. Int.* 2021,28(9): 1168-1179.
- [9] W. Gong, C. Wang, P.F. Wang, Z.H. Jiang, R. Wang, H.B. Li. Effect of La on inclusions and fracture toughness of low-alloy ultra-high-strength 40CrNi2Si2MoVA steel. *J. Iron Steel Res. Int.* 2021,28(11): 1408-1416.
- [10] H. Cui, Y.P. Bao, M. Wang, W.S. Wu. Clogging behavior of submerged entry nozzles for Ti-bearing IF steel. *Int. J. Min. Met. Mater.* 2010,17(2): 154-158.
- [11] S. Zhao, Y.Y. Ge, F.L. Zhang, et al. Optimization of refining slag composition and the deoxidation practice of liquid steel in BOF-CAS-CC process. *Trans. Indian Inst. Met.* 2020, 73(2): 497-504.
- [12] C. Wang, N. T. Nuhfer and S. Sridhar. Transient behavior of inclusion chemistry, shape, and structure in Fe-Al-Ti-O melts: effect of gradual increase in Ti. *MMTB.* 2010, 41B: 1084-1094.
- [13] J.H. Son, I.H. Jung, S. M. Jung, H. Gaye, H. G. Lee. Chemical reaction of glazed refractory with Al-deoxidized and Ca-treated molten steel. *ISIJ Int.* 2010,50(10): 1422-1430.
- [14] J.H. Son, I.H. Jung, S. M. Jung, H. Gaye, H. G. Lee. Chemical reaction of glazed refractory with Al-deoxidized molten steel. *ISIJ Int.* 2008,48(11): 1542-1551.
- [15] M.K. Sun, I. H. Jung, H. G. Lee. Morphology and chemistry of oxide inclusions after Al and Ti complex deoxidation. *Met. Mater. Int.* 2008,14(6): 791-798.
- [16] L.M. Peng, Z. Li, H. Li. Effects of microalloying and ceramic particulates on mechanical properties of TiAl-based alloys. *J. Mater. Sci.* 2006,41: 7524-7529.
- [17] C. Wang, N. T. Nuhfer and S. Sridhar. Transient behavior of inclusion chemistry, shape, and structure in Fe-Al-Ti-O melts: effect of titanium source and laboratory deoxidation simulation. *MMTB.* 2009, 40B: 1005-1021.
- [18] C. Wang, N. T. Nuhfer and S. Sridhar. Transient behavior of inclusion chemistry, shape, and structure in Fe-Al-Ti-O melts: effect of titanium/aluminum ratio. *MMTB.* 2009, 40B: 1022-1034.
- [19] W. C. Doo, D. Y. Kim, S. C. Kang and K.W. Yi. The morphology of Al-Ti-O complex oxide inclusions formed in an ultra low-carbon steel melt during the RH process. *Met. Mater. Int.* 2007, 13(3): 249-255.
- [20] S. Basu, S. K. Choudhary, N. U. Girase. Nozzle clogging behaviour of Ti-bearing Al-killed ultra low carbon steel. *ISIJ Int.* 2004, 44(10): 1653-1660.
- [21] A. Ghosh. *Secondary steelmaking: principles and applications*, 37-344; 1989, USA, CRC

Press.

[22] S. Zhao, S. P. He, Y. T. Guo, et al. Effect on cleanliness of molten steel with different refining slag systems for low alloy ship plate. *Ironmak. Steelmak.* 2016, 43(10): 790-798.

[23] X. H. Huang. *Iron and steel metallurgy principle*, 4rd edn, 314-330; 2013, Beijing, Metallurgical Industry Press.